Proceedings of the
Annual Stability Conference
Structural Stability Research Council
San Antonio, Texas, March 21-24, 2017

Experimental studies on corrugated steel plate shear walls

Qiuhong Zhao[1], Jing Qiu[2], Nan Li[3]

Abstract
Corrugated Steel Plate Shear Walls (CoSPSW) are lateral load resisting system in which corrugated steel plates are embedded inside a boundary frame, with the corrugation oriented in the horizontal or vertical direction. This paper presented experimental research on the cyclic behavior of corrugated steel plate shear walls as a new type of steel plate shear wall system. Cyclic quasi-static tests were conducted on three 1/3-scale two-story single-bay CoSPSW specimens with different corrugation orientation and different geometric properties of corrugation, and similar tests were conducted on 1/3-scale single-bay two-story SPSW specimens for comparison. All CoSPSW specimens showed highly ductile behavior and stable cyclic post-buckling performance. The specimens were able to tolerate at least 4% story drifts, and the corrugated steel panel were able to effectively improve the elastic buckling capacity and lateral stiffness of the shear wall system. The connection between the wall panel, including the flat and corrugated panels, and the boundary frame were capable of developing the full strength of the infill panel. Although hysteretic behavior of the unstiffened and corrugated specimens along with their load distribution pattern was different, eventually in all the cases, the failure of the specimen was caused by the fractures of the steel infill panels and the yielding and buckling of the bottom of columns. And the specimens all behaved as a desirable sequences of yielding: the infill panels yielded first and dissipated energy, then the boundary beams yielded and formed plastic hinges to dissipate noticeable energy, the boundary columns yielded and formed the plastic hinges at the bottom at the last. The experimental results and their implication in seismic design will be summarized and discussed.

1. Introduction

Steel plate shear walls (SPSWs), which is composed of thin infill steel panel and boundary elements, has high lateral stiffness, strength, ductility and redundancy, thus ideal for resisting the lateral loads in mid to high-rise buildings. In North America, the wall panels are prone to buckle elastically which generally will not affect the ultimate shear strength very much, since most of it relies on the large inelastic capacity from the tension field action. However, Canadian design code (CAN/CSA 2009) and American design guidelines (AISC 2010) all require that infill

[1] Professor, Tianjin University, <qzhao@tju.edu.cn>
[2] Graduate Research Assistant, PhD candidate, Tianjin University, <jqiu@tju.edu.cn>
[3] Graduate Research Assistant, Master graduate, Tianjin University, <linan_tju@126.com>

panels only resist the lateral loads, while the boundary columns of the SPSW system resist the vertical loads. In order to comply with this requirement, the steel panels should be installed or attached to the frame elements after all stories erected first. Due to the construction time limit of high-rise buildings in China, SPSWs could not wait to be installed after the floors have been in place, so the wall system has to undertake part of the gravity loads along with the lateral loads. Moreover, Chinese design code doesn't allow the infill panel to buckle during construction and at the serviceability limit states (Mathias, N. et al 2008). In addition to the gravity issues, another two major issues that arise in an unstiffened thin SPSW include large out-of-plane deformations and unpleasant sounds from the buckling of the infill panels. In addition, significant pinching sometimes appears in the hysteretic curves of unstiffened SPSWs with an attendant reduction in energy consuming capacity. Furthermore, the demands and reactions on the boundary elements increase because of the development of tension field action.

Although adding steel stiffeners or concrete panels could help to alleviate these issues to some extent, but the high labor cost and inconvenience associated with steel stiffener welding or mixing of steel and concrete trade on site. In addition, the welding residual stress and residual deformation of stiffened SPSWs should not be ignored. Inspired by the use of corrugated plates in steel girders, corrugated steel plate shear walls (CoSPSWs), in which corrugated steel plates are embedded inside a boundary frame, with the corrugation oriented in the horizontal or the vertical direction, are expected to be an improved option with solving the above issues of the unstiffened thin SPSWs without welding stiffeners or casting concrete on site.

Corrugation will form "ribs" on the wall panel, and the axial stiffness and out-of-plane bending stiffness are greatly enhanced along the direction parallel to the ribs, while the stiffness will become minimum along the direction perpendicular to the ribs, which is called "Accordion Effects". As a result, wall panels with vertical ribs or vertical corrugation (vertical CoSPSWs) will be able to resist the gravity loads transferred to them effectively due to enhanced vertical buckling capacity, while wall panels with horizontal ribs or horizontal corrugation (horizontal CoSPSWs) will neatly avoid the gravity loads transferred to them due to the "Accordion Effects". In both cases, buckling of the wall panel under gravity loads could be prevented, and the infill panels could be conveniently erected along with the boundary frame during the construction process.

Research on SPSWs with corrugated plates was quite limited, and only a number of experimental researches were carried out. Berman and Bruneau conducted cyclic tests on one-story SPSWs with unstiffened plate and inclined corrugated plate respectively. All specimens achieved significant ductility and energy dissipation, but tension field action for the CoSPSW developed only in the inclined direction, resulting in asymmetric hysteresis loops (Berman, J.W. et al 2005). Massood Mofid et al. conducted cyclic tests on one-story SPSWs with unstiffened plate, horizontal and vertical corrugated plate respectively. Test results showed that CoSPSWs had higher energy dissipation capacity, ductility and initial stiffness than SPSWs, but lower ultimate strength (Emami, F. et al 2013). And scholars of university of California at Berkeley conducted a total of 44 cyclic racking tests of corrugated sheet steel shear wall for lightly-framed multi-story residential buildings, and provided a design table listing the nominal shear strength values for corrugated sheet steel shear walls for practicing engineers (Vigh, L.G. et al 2012). But these walls has little value in the practical application of high-rise buildings.

Totally, CoSPSWs are expected to be an improved option for resisting the lateral loads in mid to high-rise buildings due to the following reasons such as higher buckling capacity, more lateral stiffness, more out-of-plane stiffness, better solution for gravity issues and faster construction. Thus, this paper presented experimental research on the cyclic behavior of corrugated steel plate shear walls as a new type of steel plate shear wall system. This paper describes the cyclic testing of a series of 1/3-scale two-story single-bay SPSW and CoSPSW specimens to study the failure mode, initial stiffness, ductility, deformation capacity, and energy dissipation capacity of the SPSWs and CoSPSWs.

2. Experimental Program

2.1 Test Specimens

The specimens were designed based on a scaled prototype building, and all the specimens were constructed in 1/3-scale, two-story and single-bay. The details of the tested specimens are shown in Fig. 1. As shown in Fig. 1, the first specimen was an unstiffened thin flat SPSW, the second specimen was the trapezoidally vertical CoSPSW with the section type I, the third one was the trapezoidally horizontal CoSPSW with the same section type I, and the fourth one was the trapezoidally horizontal CoSPSW with the section type II. The geometric properties of the corrugated panels are shown in Fig. 2. Boundary frames of the corrugated specimens were considered to be similar. Furthermore, the applied infill steel panels in all the specimens were similar that they just turned into the trapezoidal form for the corrugated specimens.

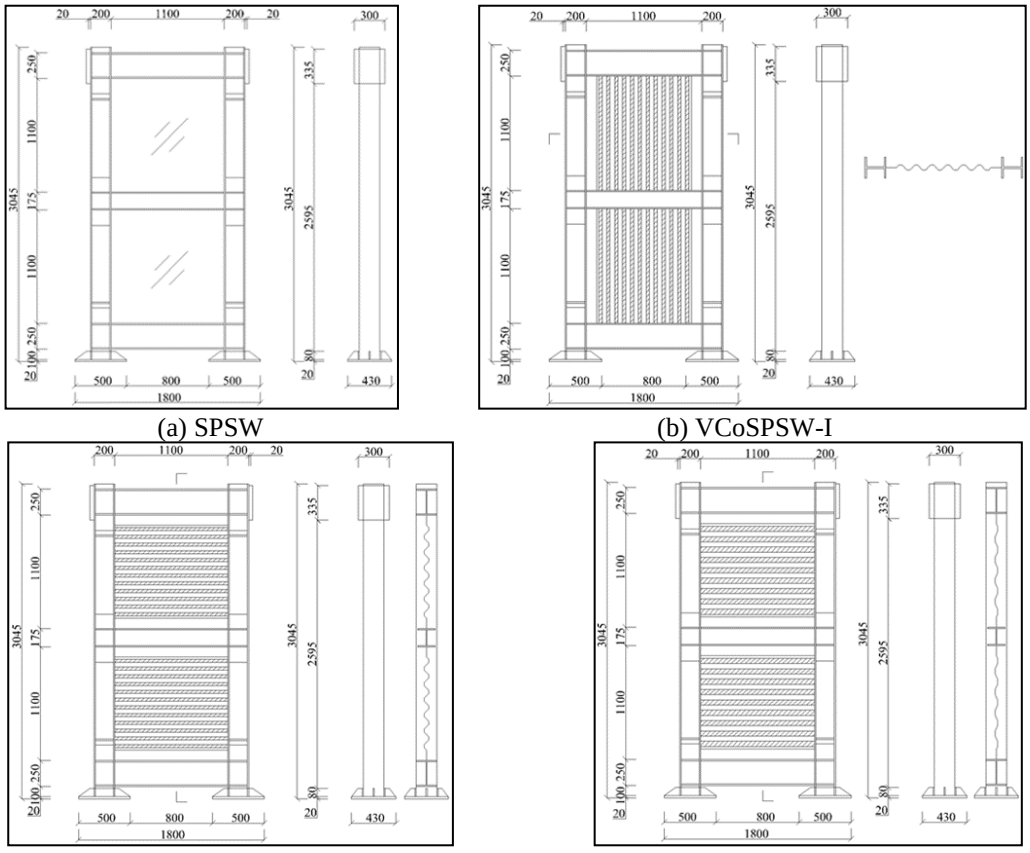

Figure 1: Test specimens

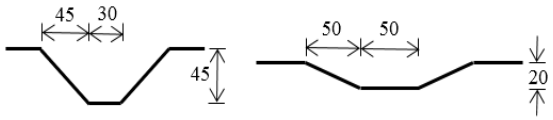

(a) Type I (b) Type II

Figure 2: Geometric properties of two types of trapezoidally corrugated plate

In each specimen, the top beam and the bottom beam section had the same dimension of H250×200×12×14, the section of the middle beam was H175×175×8×10. And the section of columns was H200×200×8×12. The dimension of the infill panel in each specimen was 1100×1100 with thickness of 2mm. In addition, the details of beam-to-column connection and panel-to-boundary connection of unstiffened flat specimen and corrugated specimens are shown in Fig. 3. It has to be mentioned that the connection between the straight edge of the corrugated panel and the boundary frame was the same as the unstiffened flat panel.

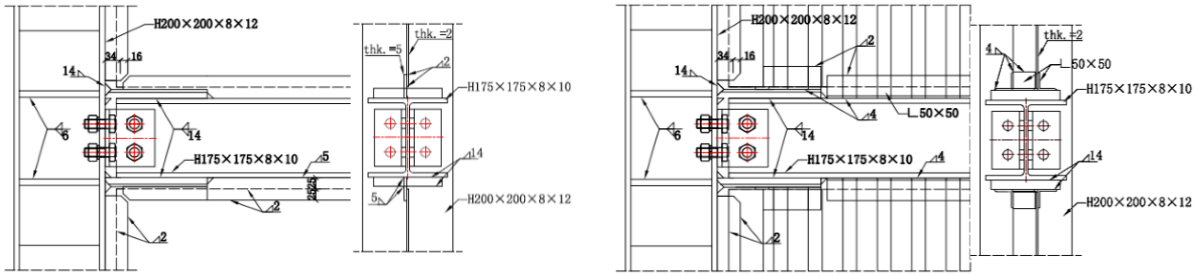

Figure 3: Details of the connections

2.2 Material Properties

Material properties specified for the specimens consisted of Q345 steel for the boundary frame members and Q235 steel for the infill panels. The material properties were determined by coupon test, and the results are listed in Table 1.

Table 1: Coupon test results

Member	Elastic modulus(1) (GPa)	Yield stress(2) (MPa)	Ultimate stress(3) (MPa)	Yield strength ratio(4)=(3)/(2) /
Infill panel	170.3	290.59	431.13	1.48
Midbeam web	196.3	386.60	551.90	1.43
Midbeam flange	192.3	345.27	478.27	1.39
Top/botbeam web	206.7	418.57	542.73	1.30
Top/botbeam flange	182.0	345.60	519.13	1.50
Column web	181.0	348.38	511.15	1.47
Column flange	203.0	320.33	494.40	1.54

2.3 Test Setup and Instrumentation

A schematic of the test setup are shown in Fig. 4. The laboratory was equipped with a reaction wall, a reaction steel frames and a strong base significantly stiffer than the specimens. The reaction wall was used for the application of the lateral loads. The reaction frame was employed for the lateral support of the specimens. Each specimen was mounted on the strong floor through an anchorage beam. Each test was performed under fully reversed cyclic quasi-static loading in the elastic and inelastic response zones of the specimens. The in-plane (west-east) cyclic loads were applied on the specimens by means of a hydraulic jack with 2,000kN capacity. In order to

prevent the out-of-plane movement, lateral support was provided at the height near the beam-to-column joint of the top beam.

A number of displacement transducers were put on the specimens to measure the global as well as local displacements of points of interest on the specimens, as shown in Fig. 4. In this way, movement of the members were monitored and important data such as shear wall panel deformation, out-of-plane displacement of the infill panel and rotation of the beam and column could be measured. In order to measure strains at various critical locations on the specimens, linear as well as "rosette" strain gauges were mounted to the specimens.

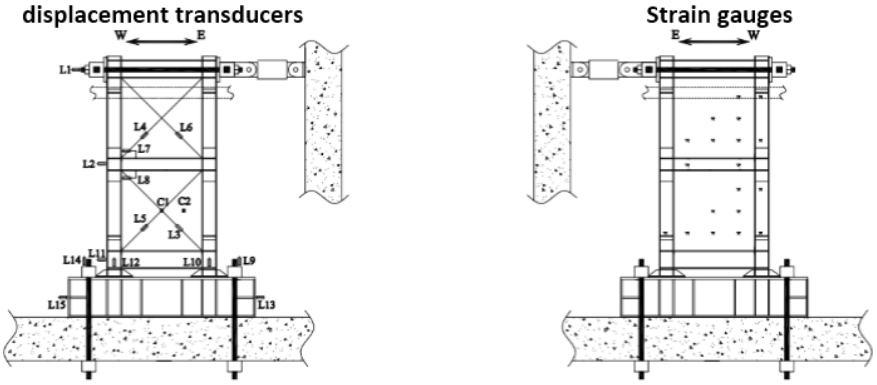

Figure 4: Test setup and instrumentations

2.3 Loading Protocol

The lateral loads were imposed using the combination of load-control scheme and displacement-control scheme, as shown in Fig. 5. The detailed loading procedure was as follows: (1) the lateral loads were applied using a load-control scheme and the spacing between each control point was 100kN before the yielding of specimens and repeated only once at each control point; (2) the lateral loads were imposed using a displacement-control scheme and the spacing between each control point is 0.25% drift after the yielding of specimens that could be known when an inflection appeared in the load-drift curves and repeated twice at each control point; and (3) the spacing between each control point improved to 0.5% drift after the load drift reached 2.0%. When the lateral load dropped below 85% of the maximum load or the load drift arrived at the 5%, the test was stopped. In this study, due to the limited equipment in the laboratory, the hydraulic jacks used to provide the cyclic load were controlled by the laboratory technicians. Therefore, the load frequency was not controlled automatically, and consequently load sequence was somewhat an approximate value.

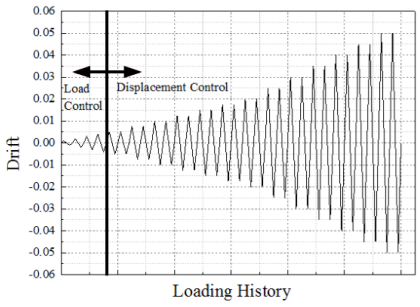

Figure 5: Loading protocol

3. Experimental Results

The variations of stiffness, ultimate strength, ductility, and energy dissipation capacity are the main characteristics which affect the seismic performance of the steel plate shear wall. In this experimental research, for each specimen, loading was stopped when the value of the wall strength dropped to 85% of their ultimate strength with increasing displacement amplitude, or when displacement amplitude reached 5% total drift. Hysteretic behaviors of all the specimens are shown in Fig. 6. Further, Fig. 7 indicates the typical deformation pattern after the structural testing. Although hysteretic behavior of the unstiffened and corrugated specimens along with their load distribution pattern was different, eventually in all the cases, the failure of the specimen was caused by the fractures of the steel infill panels and the yielding and buckling of the bottom of columns. And the specimens all behaved as a desirable sequences of yielding: the infill panels yielded first and dissipated energy, then the boundary beams yielded and formed plastic hinges to dissipate noticeable energy, the boundary columns yielded and formed the plastic hinges at the bottom at the last. In other words, the design principles of these steel plate shear walls were satisfied for all of these four specimens. The following are the discussions of the experimental loading.

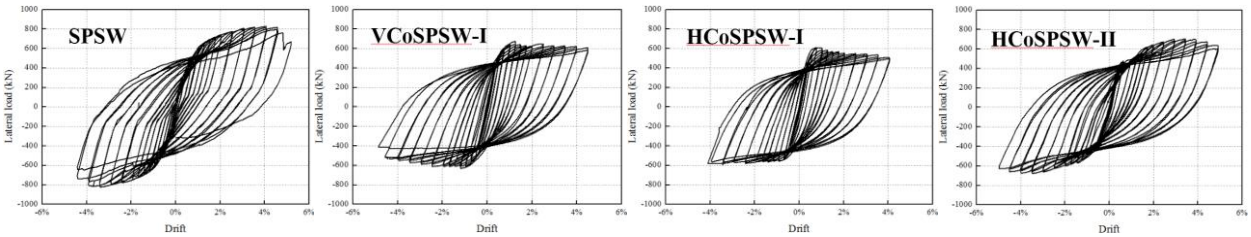

Figure 6: Hysteresis curves of the tested specimens

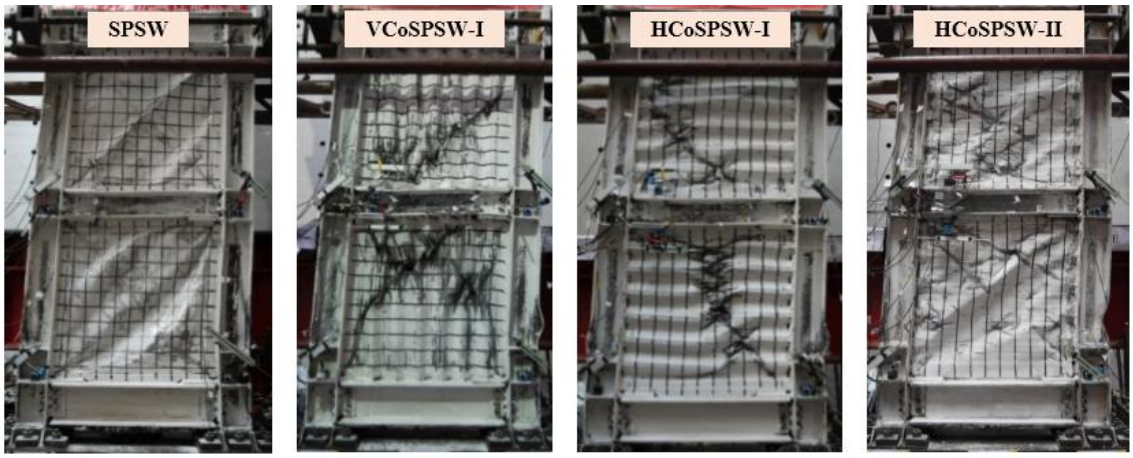

Figure 7: State of specimens at ultimate stage

3.1 Cyclic Behavior of Specimen SPSW

Specimen SPSW, with unstiffened flat infill panels, behaved in a ductile and desirable manner. Up to overall lateral load of about 300kN, the specimen was almost elastic. At lateral load of about 300kN, the compression diagonal in the infill steel panels was buckling and then diagonal tension field was forming gradually. The specimen could tolerate 29 cycles, out of which 22 were inelastic, before reaching an overall drift of 0.05 and maximum shear strength of about 828.15kN. At this level of drift, fractures were wide-spread in the infill panels (due to low-cycle fatigue), the longest cracks at the middle of the infill panel extended to over 200mm. The

boundary beam was heavily yielded, the yielding of the column almost expanded into the whole height and the bottom of the boundary columns yielded and distorted heavily. Shear strength of the specimen dropped to lower than 85% of the maximum capacity of the specimen, and the specimen was considered failed. The test stopped.

There was no obvious phenomenon at the specimen that the surface of the infill steel plate still remained smooth before 300kN. In this period, the hysteresis loops was almost linear, so the area surrounded by the hysteresis loops was still close to zero. And the maximum out-of-plane displacement of the infill panel was only 0.8mm. Elastic buckling of the infill panel was observed during the loading process of the 300kN, at this time, the lateral displacement reached about 4mm (0.3% drift). The buckling shape was diagonally formed, and the maximum out-of-plane displacement of the infill panel suddenly reached 5.1mm. Slight diagonal yielding in tension was observed at the edge of the infill panel near the corner. For the boundary frame, very slight yielding short lines was detected at the bottom outer side of the column flange. With the increase of the loading displacement amplitude, the yielded areas on the infill panel and the boundary beams and columns grew larger. The infill panel buckled accompanied with several loud bangs, and these noises occurred in each cycle as the panel buckled popped through and reoriented themselves upon reversal of the loading direction. The first crack was detected during the loading process of 1.25% drift at the top corner of the infill panel. It formed due to the low-cycle fatigue and stress concentration and located near the weld connecting the infill panel to the fish plate. By continuing the loading, the cracks at the infill panel increased both in number and dimension. In the cycle of 2.5% drift, the web and flange of the middle beam was severely yielded that the plastic hinge was considered had been formed. And in the cycle of 4% drift, the distortion of the column flange was observed at the bottom end, and the lateral bearing capacity started to go down until the shear strength dropped to lower than 85% of the maximum capacity.

3.2 Cyclic Behavior of Specimen VCoSPSW-I

Specimen VCoSPSW-I, with vertical-oriented corrugated infill panels with type I geometric property of deeper groove, behaved in a ductile and desirable manner. Up to overall lateral load of about 500kN, the specimen was almost elastic. At lateral load drift of about 1.25%, after the yielding almost spread to the whole panel, the inelastic buckling occurred at the infill panel. The specimen could tolerate 30 cycles, out of which 24 were inelastic, before reaching an overall drift of 0.045 and maximum shear strength of about 672.76kN. At this level of drift, fractures were wide-spread at the intersections of the buckling shape in the infill panels (due to low-cycle fatigue), the longest cracks at the middle of the infill panel extended to over 200mm. The boundary beam was heavily yielded, and the bottom of the boundary columns yielded and distorted heavily. Shear strength of the specimen dropped to lower than 85% of the maximum capacity of the specimen, and the specimen was considered failed. The test stopped.

There was no obvious phenomenon at the specimen that only very slight yielding spots were detected at the bottom of the column flange before 400kN. In this period, the hysteresis loops was almost linear, so the area surrounded by the hysteresis loops was still close to zero. In the cycle of 400kN, slight yielding lines was detected at the edge of the corrugated infill panel near the boundary frame. Combined with the strain data measured by the “rosette” strain gauges mounted to the infill panels, the yielding of the infill panels almost expanded to the whole panel with the increase of the load amplitude. By increasing load and displacement amplitude, the

yielding lines of the infill panel became more instinct, and the yielding area of the middle beam and the bottom of the column web grew larger. In the cycle of 1.25% drift, inelastic buckling of the corrugated infill panel was observed during the loading process, the buckling shape crossed 3 waves and was almost symmetrical in different loading direction. And at this state, the maximum shear strength was reached. With the increase of the loading displacement amplitude, the yielded areas on the infill panel and the boundary beams and columns grew larger. The first crack was detected during the loading process of 2.0% drift. It formed due to the low-cycle fatigue and located at the intersections of the buckling shape of the infill panel. By continuing the loading, the cracks at the infill panel increased both in number and dimension. In the cycle of 3.0% drift, the web and flange of the middle beam was severely yielded that the plastic hinge was considered had been formed. And in the cycle of 3.5% drift, the distortion of the column flange was observed at the bottom end, and the lateral bearing capacity continued going down until the shear strength dropped to lower than 85% of the maximum capacity.

3.3 Cyclic Behavior of Specimen HCoSPSW-I

Specimen HCoSPSW-I, with horizontal-oriented corrugated infill panels with type I geometric property of deeper groove, behaved in a ductile and desirable manner. Up to overall lateral load of about 450kN, the specimen was almost elastic. At lateral load drift of about 1.0%, after the yielding almost spread to the whole panel, the inelastic buckling occurred at the infill panel. The specimen could tolerate 28 cycles, out of which 22 were inelastic, before reaching an overall drift of 0.04 and maximum shear strength of about 610.19kN. At this level of drift, fractures were wide-spread at the intersections of the buckling shape in the infill panels (due to low-cycle fatigue), the longest cracks at the middle of the infill panel extended to over 150mm. The boundary beam was heavily yielded, and the bottom of the boundary columns yielded and distorted heavily. Shear strength of the specimen dropped to lower than 85% of the maximum capacity of the specimen, and the specimen was considered failed. The test stopped.

The behavior during the loading process was similar with the specimen VCoSPSW-I. There was no obvious phenomenon at the specimen that only very slight yielding spots were detected at the bottom of the column flange before 450kN. In this period, the hysteresis loops was almost linear, so the area surrounded by the hysteresis loops was still close to zero. In the cycle of 450kN, slight yielding lines was detected at the edge of the corrugated infill panel near the boundary frame. Combined with the strain data measured by the “rosette” strain gauges mounted to the infill panels, the yielding of the infill panels almost expanded to the whole panel with the increase of the load amplitude. By increasing load and displacement amplitude, the yielding lines of the infill panel became more instinct, and the yielding area of the middle beam and the bottom of the column web grew larger. In the cycle of 1.0% drift, inelastic buckling of the corrugated infill panel was observed during the loading process, the buckling shape crossed 3 waves but the buckling shape was not symmetrical with that in different loading direction. And at this state, the maximum shear strength was reached. With the increase of the loading displacement amplitude, the yielded areas on the infill panel and the boundary beams and columns grew larger. The first crack was detected during the loading process of 1.75% drift. It formed due to the low-cycle fatigue and located at the intersections of the buckling shape of the infill panel. By continuing the loading, the cracks at the infill panel increased both in number and dimension. In the cycle of 2.5% drift, the web and flange of the middle beam was severely yielded that the plastic hinge was considered had been formed. And in the cycle of 3.5% drift, the distortion of the column

flange was observed at the bottom end, and the lateral bearing capacity continued going down until the shear strength dropped to lower than 85% of the maximum capacity.

3.4 Cyclic Behavior of Specimen HCoSPSW-II

Specimen HCoSPSW-I, with horizontal-oriented corrugated infill panels with type II geometric property of shallower groove, behaved in a ductile and desirable manner. Up to overall lateral load of about 400kN, the specimen was almost elastic. At lateral load of about 400kN, the infill panel buckled elastically, then the corrugation was flattened and the tension field action formed gradually. The specimen could tolerate 30 cycles, out of which 24 were inelastic, before reaching an overall drift of 0.05 and maximum shear strength of about 704.93kN. At this level of drift, the original corrugation was no longer apparent and fractures were wide-spread at the intersections of the buckling shape and the original corrugation in the infill panels (due to low-cycle fatigue), the longest cracks at the middle of the infill panel extended to over 130mm. The boundary beam was heavily yielded, and the bottom of the boundary columns yielded and distorted heavily. Shear strength of the specimen dropped to about 85% of the maximum capacity of the specimen, and the drift reached 0.05 so the specimen was considered failed. The test stopped.

The behavior during the loading process was similar with the specimen HCoSPSW-I before buckling of the corrugated panels and similar with the specimen SPSW after the formation of the tension field action. There was no obvious phenomenon at the specimen that only very slight yielding spots were detected at the bottom of the column flange before 400kN. In this period, the hysteresis loops was almost linear, so the area surrounded by the hysteresis loops was still close to zero. In the cycle of 400kN, elastic buckling of the corrugated panel was occurred. The buckling shape crossed one and a half wave and fade away in the process of the loading of another direction. And at this state, slight yielding also was detected at the edge of the corrugated infill panel near the boundary frame. By increasing load and displacement amplitude, the buckling and yielding lines of the infill panel became wider and more instinct, and the yielding area of the middle beam and the bottom of the column web grew larger. Noises also created due to the deformation of the infill panel, but were much less than the specimen SPSW. With the flattening of the corrugated panel, the growth rate of the shear strength was increased again. The first crack was detected during the loading process of 1.75% drift. It formed due to the low-cycle fatigue and located at the intersections of the buckling shape of the infill panel and also at the corner between the infill panel and the fish plate. By continuing the loading, the cracks at the infill panel increased both in number and dimension. In the cycle of 2.5% drift, the web and flange of the middle beam was severely yielded that the plastic hinge was considered had been formed. And in the cycle of 3.5% drift, the distortion of the column flange was observed at the bottom end, and the lateral bearing capacity started to go down until the shear strength dropped to lower than 85% of the maximum capacity.

3.5 Elastic and Inelastic behavior

Utilizing the experimental results of these four specimens under cyclic in-plane loading, the lateral load-top displacement skeleton curves of specimen SPSW and CoSPSW specimens are shown in Fig. 8. Compared with CoSPSW specimens, there is no obvious turning points on skeleton curve of specimen SPSW while the buckling points of corrugated infill panel are the distinct turning points on skeleton curves of specimen VCoSPSW-I and HCoSPSW-I. That is because the buckling of flat infill panel occurred early and then the tension field action gradually

formed, the bearing capacity of specimen SPSW increased with the increase of the lateral displacement continuously. However, for the specimen VCoSPSW-I and HCoSPSW-I, the corrugated infill panel bore lateral load with relatively higher stiffness until the panel buckled at a relatively higher lateral capacity, and at this stage, the yielding of the corrugated infill panel almost expanded to the whole panel, so once the buckling occurred, the lateral capacity of the infill panel would decreased, thus formed a distinct turning point on the load-drift curve. For the specimen HCoSPSW-II, the buckling of the corrugated panel occurred before the yielding expanded to the whole panel, so the turning point occurred earlier than CoSPSW-I specimens. And with the increase of the lateral displacement, the tension field action gradually formed, so the carrying capacity rose again.

Although, compared with the other two specimens, the behavior of two CoSPSW-I specimens were similar, they still had differences. Specimen HCoSPSW-I was buckled earlier than the specimen VCoSPSW-I at a relatively smaller drift with lower lateral load. So the maximum lateral load of HCoSPSW-I was lower than specimen VCoSPSW-I as the turning point was the maximum lateral load of CoSPSW-I specimens. And it should be pointed out that, although the load displacement curve of these two specimens began to decline after the buckling of the infill panels, the decrease was limited.

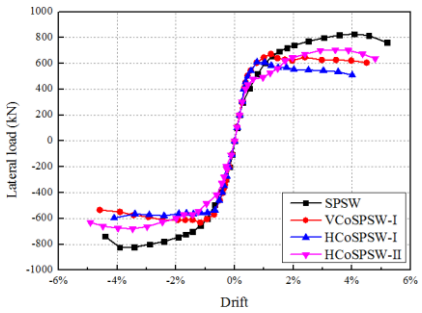

Figure 8: Skeleton curves of the tested specimens

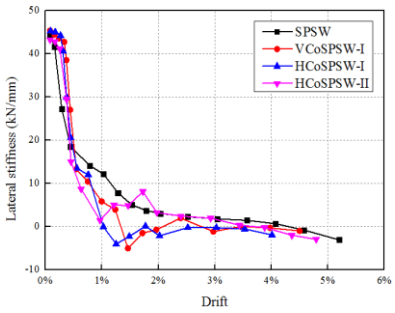

Figure 9: Lateral stiffness

The differences of these specimens' behaviors could also be observed in the stiffness curves shown in Fig. 9. The stiffness of specimen SPSW decreased rapidly from the beginning since its early buckling. Then, after buckling with the increase of the lateral displacement, the infill panel began to yield in diagonal direction and the tension field formed gradually. At last, boundary elements began to yield until the total ultimate capacity was reached. For specimen VCoSPSW-I or HCoSPSW-I, the initial stiffness of CoSPSW-I specimens kept in a higher level than specimen SPSW did, but decreased quickly as the infill panel began to yield. After the yielding had extended to the whole infill panel, the descending rate became slower until the inelastic buckling of the corrugated infill panel occurred, which occurred earlier of specimen HCoSPSW-I than specimen VCoSPSW-I. And with the inelastic buckling of the infill panel, the lateral capacity of the infill panel decreased significantly, which led to a negative value of the stiffness. At last, with the yielding of the boundary elements, the stiffness kept around zero. For specimen HCoSPSW-II, the stiffness began to decline earlier than CoSPSW-I specimens but later than specimen SPSW, and the stiffness curve declined at a relatively fast rate continuously. But different from other specimens, the stiffness began to rise again at a relatively larger lateral displacement. The reason is that the tension field gradually formed with the increase of the lateral displacement. At last, the boundary elements began to yield until the total ultimate capacity was reached.

3.6 Ductility and Energy Dissipation

Deformability and the amount of energy dissipated under seismic load are major parameters in the lateral load resisting systems. As it was illustrated in Fig. 6, although all the specimens dissipate the energy with stable hysteresis loops, there was pinching in the hysteresis loops of the specimen SPSW. Both of the CoSPSW-I specimens were able to dissipate more energy compared to the unstiffened flat specimen. There was also slight pinching in the hysteresis loops of specimen HCoSPSW-II, but with a significant improvement compared with the specimen SPSW. In order to better illustrate the differences, Fig. 10 shows the hysteresis loop at 1.5% drift of the specimens, and the superiority of CoSPSW specimens are distinct.

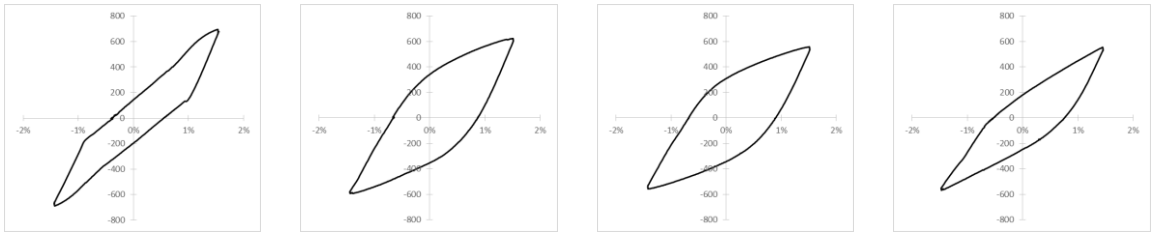

(a) SPSW (b) VCoSPSW-I (c) HCoSPSW-I (d) HCoSPSW-II

Figure 10: Hysteresis loops at 1.5% drift of tested specimens

The cumulated energy curves were illustrated in Fig. 11. The steel plate shear walls are suggested to remain elastic at frequent earthquake state and permit shear panel yield at moderate earthquake. So, as shown in Fig. 11, the specimens dissipated energy mainly at a relatively larger drift. The cumulated energy dissipation of CoSPSW-I specimens were higher than specimen SPSW and HCoSPSW-II, and specimen VCoSPSW-I and HCoSPSW-I dissipate nearly the same energy in different drift. The capacity and ductility of the tested specimens are summarized in Table 2. The yield load P_y and yield displacement Δ_y were calculated according to the method shown in Fig. 12. As mentioned before, although the ultimate strength of the unstiffened flat specimen was larger than that of the corrugated specimens, the stiffness, ductility ratio and energy dissipation of the corrugated specimens were larger than those of the unstiffened specimen.

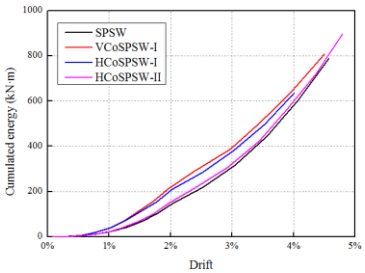

Figure 11: Cumulated energy of tested specimens

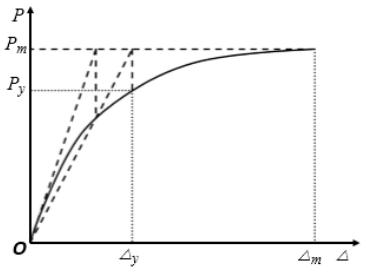

Figure 12: Calculation sketch of P_y & Δ_y

Table 2: Summary of test results

Specimens	P_y(1) kN	Δ_y(2) mm	Stiffness(3)= (1)/(2) kN/mm	P_m(4) kN	Δ_m(5) mm	Δ_u(6) mm	Ductility ratio(7)= (6)/(2)
SPSW	632.5	33.33	18.98	828.2	116.1	148.1	4.4
VCoSPSW-I	577.3	18.66	30.94	672.8	35.30	128.3	6.9
HCoSPSW-I	559.8	17.46	32.07	610.2	21.67	114.3	6.6
HCoSPSW-II	487.6	24.82	19.65	704.9	97.86	136.6	>5.5

3.7 Out-of-plane Displacement of the Infill Panels

Fig. 13 shows the out-of-plane displacements of the infill panels of test specimens at different load level. Due to the quantity limit, only two cable displacement meters were arranged at the infill panel of lower story of every specimen, as shown in Fig. 4. This arrangement could almost represent the position of the maximum out-of-plane displacement in the panel. As shown in Fig. 13, the unstiffened flat panel underwent large out-of-plane displacement at relatively lower load level, and the corrugation could constraint the out-of-plane displacement effectively. This advantage of corrugated panels could also be obtained in Fig. 7. The corrugated panel of specimen HCoSPSW-II underwent notably larger out-of-plane displacement compared with other corrugated panels at relatively higher load level. But it needs to be explained that the corrugated plate itself was not in a plane before loading, so even the result of the out-of-plane displacement of this panel was high, but the corrugated plate was gradually flattened in fact, rather than stick out from the original surface. The remarkable superiority of the out-of-plane displacement is of great significance for the practical application that the infill panels should ensure not to buckle and develop much out-of-plane deformation accompanied with several loud noise in serviceability limit state, such as under wind load. In other words, the corrugated panel could improve the serviceability of the steel plate shear wall system.

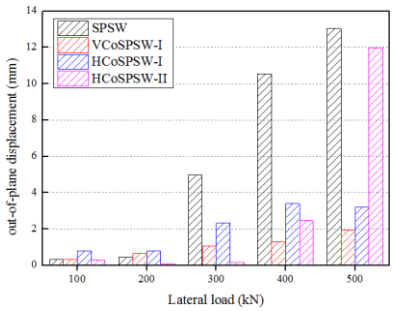

Figure 13: Out-of-plane displacements of infill panel at different load level

3. Conclusions

In this research, three one-third scaled CoSPSW specimens and one conventional unstiffened SPSW specimen were designed and tested using quasi-static loading to investigate the performance of corrugated steel plate shear walls. Two of the corrugated specimens had corrugated panels with the type I geometric property, one horizontal-oriented and one vertical-oriented, while the third corrugated specimen was assembled with corrugated panels with the type II geometric property and also horizontal-oriented. The behaviors of these different specimens were compared, and the following conclusions can be drawn: Firstly, all the specimens showed high ductility during the test. The specimens reached a maximum story drift of at least 0.04 when they failed and dropped to 85% of their shear capacities. And these four specimens all behaved as a desirable sequences of yielding that the infill panels yielded and dissipated energy before the boundary beams and columns. Then, the corrugated specimens showed higher buckling stability, out-of-plane stiffness and lateral stiffness, especially the ones with the type I geometric property of deeper groove. Although the ultimate strength of the unstiffened specimen was larger compared to that of the corrugated specimens, the corrugated specimens were able to yield at a relatively larger drift and dissipate energy through plastic deformation without any pinching in the hysteretic loops. And the ductility ratio of the corrugated specimen was larger than the unstiffened specimen. In a word, the corrugated specimens could solve the major issues that arise in an unstiffened thin SPSW effectively as

expected. Last, the behavior of the corrugated specimens was not greatly affected by changing the corrugation direction, but greatly affected by changing the geometric property of deeper or shallower groove. So further investigation of the better type selection for the corrugated panels was quite necessary in the future study.

Acknowledgments

The authors of this paper would like to express their appreciation for the financial support given by the Nature Science Foundation of China (No. 51378340) and the Specialized Research Fund for the Doctoral Program of Higher Education, China (SRFDP: 20130032120055). Support from the funding agency above is gratefully acknowledged.

References

Canadian Standards Association. (2009). "Limit states design of steel structures." *CAN/CSA S16-2009*.

American Institute of Steel Construction. (2010). "Seismic provisions for structural steel buildings." *ANSI/AISC 341-2010*.

Mathias, N., Sarkisian, M., Long, E., Huang, Z. (2008). "Steel plate shear walls: efficient structural solution for slender high-rise in China." *American Institute of Physics*, 1020(1) 43-50.

Berman, J.W., Bruneau, M. (2005). "Experimental investigation of light-gauge steel plate shear walls." *Journal of Structural Engineering*, 131(2) 259-267.

Emami, F., Mofid, M., Vafai, A. (2013). "Experimental study on cyclic behavior of trapezoidally corrugated steel plate shear walls." *Engineering Structures*, 48(48) 750-762.

Vigh, L.G., Deierlein, G.G., Miranda, E., Liel, A.B., Tipping, S. (2012). "Seismic performance of steel corrugated shear wall" *Research Report*, Stanford University.